

Comparative Analysis between a Discrete Spiral Chamber and a Continuous Spiral Chamber via ANSYS

Análisis Comparativo entre Una Cámara en Espiral Discreta y Continua Via Ansys

Carlos Andrés Sánchez-Ríos ^{1*}, Jonathan Graciano-Uribe ¹, Sebastián Vélez García ¹, Diego Andrés Hincapié-Zuluaga ¹

¹ Instituto Tecnológico Metropolitano, Medellín, Colombia

Received: 21 Oct 2015

Accepted: 18 Feb 2017

Available Online: 27 Feb 2017

Abstract

Hydraulic turbines have been elements of utmost importance to meet the energy needs of communities worldwide. These are used with elements that improve the flow behavior of water to the turbine so that its energy benefits are improved. Spiral chambers are circular elements where their cross-section is constantly changing and are used in reaction turbines, such as Francis turbines. Their main function is to distribute evenly the fluid into the impeller inlet. This paper sought to use engineering simulation tools (ANSYS - CFX) to compare behavior and performance from a discrete continuous spiral chamber in a virtual environment under the same physical operating conditions, providing a comparative view of the performance present between the two manufacturing methods of spiral chambers.

Keywords: Spiral chamber, Reaction Turbine, ANSYS - CFX, Francis Turbine Micro Generators, Hydrodynamic Simulation, Blade Position, Kaplan Turbine

Resumen

Las turbinas hidráulicas han sido un elemento de alta importancia para suplir las necesidades energéticas de las comunidades a nivel global, éstas son empleadas en conjunto con elementos que mejoren el comportamiento del flujo de agua hacia la turbina de tal manera que se mejoren las prestaciones energéticas de la misma. Las cámaras en espiral son elementos circulares donde su sección transversal varía constantemente y son empleadas en turbinas de reacción, como las turbinas Francis, su función principal es distribuir uniformemente el fluido en la entrada del rodete, éste trabajo busca emplear herramientas ingenieriles de simulación (Ansys - CFX) para generar una comparativa del comportamiento y prestaciones entre una cámara en espiral discreta y una continua, en un entorno virtual bajo las mismas condiciones físicas y de operación, aportando una vista comparativa al rendimiento que se puede presentar entre los dos métodos de fabricación de las cámaras en espiral

Palabras clave: Cama en Espiral, Turbina de Reacción, Ansys – CFX, Turbina Francis.

1. Introduction

One way of producing electricity is through hydroelectric plants, which use the interaction of a mobile vane with a fluid in motion and, consequently, changes the amount of movement between the vane and the stream generate forces

that work through the vane's displacement [1]. Said hydraulic turbines are classified with respect to their operating characteristics and geometry, as shown in Fig.1.

*Corresponding Author.

E-mail: carlossanchez1307@gmail.com

How to cite: Sanchez, C., Graciano, J., Velez, S., Zuluaga, D., *Comparative Analysis between a Discrete Spiral Chamber and a Continuous Spiral Chamber via ANSYS*, TECCIENCIA, Vol. 12 No. 23, 29-38, 2017.

DOI: <http://dx.doi.org/10.18180/tecciencia.2017.23.4>

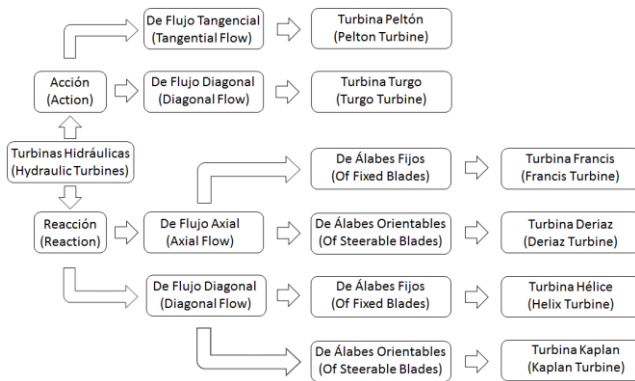


Figure 1 Classification of hydraulic turbines. Adapted from [1].

According to the flow conditions (Q) and pressure head (H), it is possible to select the type of turbine to implement, through any of the existing selection abacuses [2], [3]. Figure 2 is an example of one of these abacuses; therein, it can be noted that the Francis-type turbine has a broad range of operation, making it worthy of study.

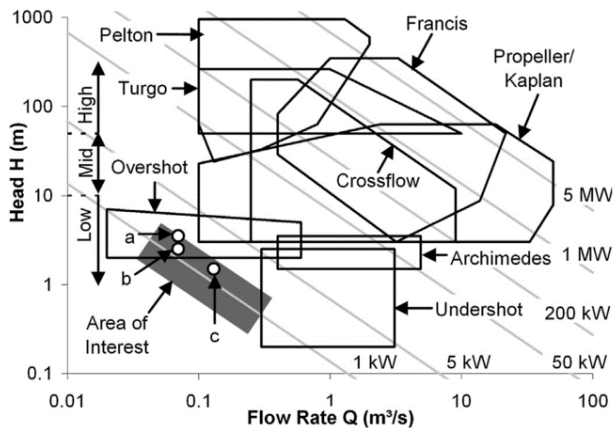


Figure 2 Turbine selection abacus. Taken from [2].

Francis-type turbines are comprised of a runner, draft tube, stay vanes, wicket gate, and the spiral chamber (casing) [4].

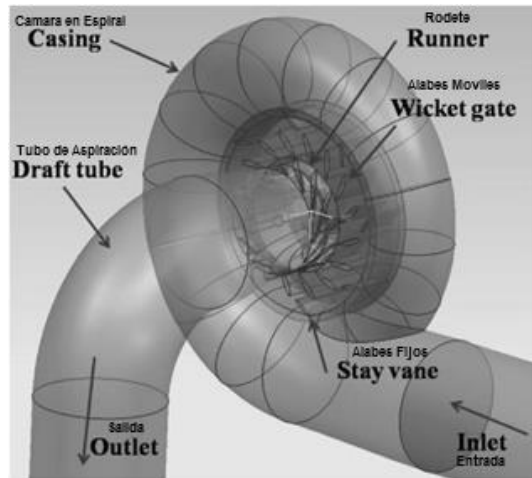


Figure 3 Francis turbine coupled with a spiral chamber

Spiral chambers are vitally important constitutive elements in the structure of hydraulic reaction turbines (Francis, Kaplan, propeller, and Deriaz) and are in charge of distributing water throughout the runner’s periphery of said turbines [5]. In turn, these are in charge of changing the linear flow reaching the chamber inlet into radial and tangential flow, which will be delivered to the chamber outlet to be used by the turbine’s vanes. During the interaction process between the fluid and the turbine, an exchange exists of the linear and angular moment of the axis moment and rotational speed pair in the turbine shaft, where the product between these last two amounts is the shaft power.

In spite of their proven importance in the generation of electric power, their design and construction is still precarious. Their design is achieved through trial and error in empirical practice, which implies high costs and in most cases inefficient designs. However, other methods have been applied for their design, for example, an analysis has been performed of the spiral chambers, starting with the potential flow theory, which is a valid approach in this case due to the irrotationality of the flow, as shown in the lines of current or streamlines obtained numerically by several studies [4], [6]–[8]. In their design, least squares regressions have also been used [3], [5]. Additionally, the experimental analysis of the spiral chambers is normally conducted indirectly, given that what is analyzed is the turbine’s global behavior [9].

This work sought to compare two geometries of spiral chambers, one continuous and the other sectioned, and evaluate the velocities obtained for each at the outlet.

2. Methodology

This project was structured into three stages. Initially, a design was made of the computational model of the spiral chamber, then, the system was simulated in Ansys® CFX; finally, the results are analyzed and discussed.

2.1 Computational model of the spiral chambers

The computational model for each of the chambers was carried out under different CAD environments; the following provide details of each of the processes:

2.1.1. Spiral-sectioned chamber

The computational model for the spiral-sectioned chamber was elaborated in the Siemens NX® 10.0 program, starting from a series of descriptive plans of real spiral chamber, measurements from which the chamber thickness was subtracted to achieve a representative volume of the water flow within the chamber. The spiral chamber's principal measurements are outlet diameter of 2.0 m and central diameter of 2.322 m.

Upon taking the measurements and making calculations through least squares regressions – as already done in methods, like that exposed by Professor Stefan Zarea [3], [5], a two-dimensional sketch was made of the chamber's internal volume (Fig. 4). Then, cross-sections were drawn with the corresponding diameters of the different sections (Fig. 5). Once the process was finished, a set of surfaces was generated on each of the sections of the geometry; given that these surfaces are closed entities, they generate a solid volume upon ending the operation (Fig. 6) until having a complete reconstruction of the radial geometry of the spiral chamber's internal water volume (Fig. 7).

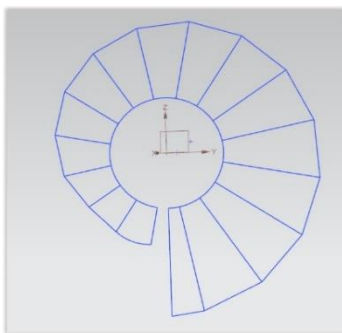


Figure 4 2D drawing

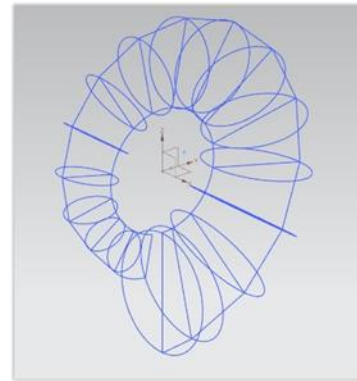


Figure 5. 2D drawing with diameters in the cross-sections

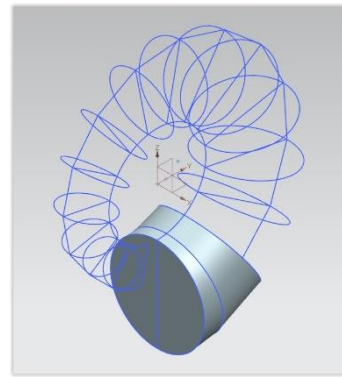


Figure 6 Generation of surfaces

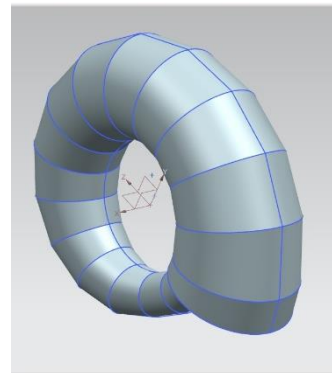


Figure 7 Sectioned surfaces

The final design step extracted the inlet section (Fig. 8) and the flow outlet ring (Fig. 9). When all the geometry sections and their components were ready, all the bodies were combined, so that the final product was the volume of the computational model. This is exported in the .IGS format, which is a format used to exchange models and surfaces among multiple CAD programs; in our case, the destiny program is Ansys® 16.02, a specialized application in computational analysis of different physical conditions.

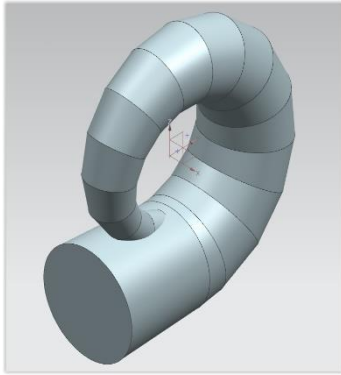


Figure 8 Chamber with inlet section.

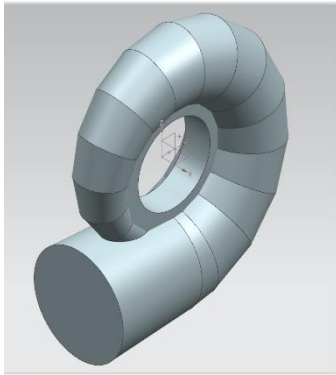


Figure 9 Chamber with interior ring

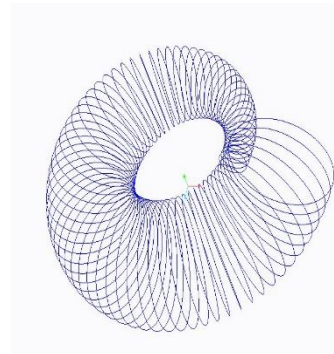


Figure 10 Cross-section of curves

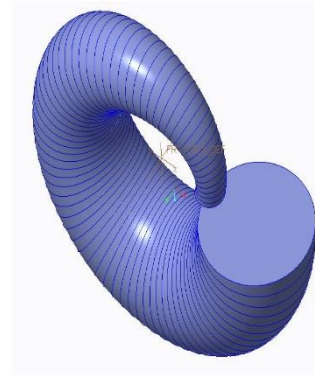


Figure 11 Final surface

A1. Continuous-spiral chamber

A computational code developed in Mat lab® was applied for the continuous-spiral chamber, which travels radially the geometry and generates curves of different cross-sections. It is only necessary to indicate the inlet radius and the internal radius of the spiral chamber, these values were the same used to design the sectioned-spiral chamber. Upon ending the process, this program generates a file with the .IBL extension ready to be imported to a CAD program, said computational code is based on the equiangular spiral where programming of said codes helps to reduce design time and improve its precision [10], [11].

The curves were imported to the PTC Creo® 3.0 program (Fig. 10) and a mix of limits was conducted on the curves and a pair of surfaces on the chamber inlet and outlet to create the principal model (Fig. 11). Thereafter, the set of surfaces was solidified and the inlet section and outlet ring were generated (Fig. 12). Finally, the volume of the computational model was exported to the .IGS format ready to be taken to Ansys® 16.02.

B. Hydrodynamic simulation of the system

This part of the work has two stages: discretization of the geometry and dynamic fluid analysis. In the first stage, the geometries are discretized in such a manner that a mesh is generated composed of a series of mathematical equations that permit the analysis module to recognize the geometry and the zones of interest. The second stage conducts a dynamic fluid analysis, which defines the physical conditions of standard behavior for both models.

B1. Discretization of the geometry

The finite volume method (FVM) involves a spatial discretization of the domain using a mesh. The mesh is used as constructor of finite volumes in which the equations are applied [13]. In this case, the Ansys® 15.0 software meshing module is used to implement the FVM. This module generates a discretization of total volumes into smaller volumes, which permit evaluating the Navier-Stokes equations on fluid dynamics. The use of advanced meshing methods permits said discretization to comply with the parameters that facilitate the simulation convergence; said parameters include obliquity, whose values range between zero and one, which seek for the maximum value to be as far

as possible from the upper limit. The maximum value of the aspect ratio is recommended to be <30 ; the maximum value for the orthogonal quality is required as close as possible to one. Table 1 shows the values corresponding to the metrics of each meshing.

Both geometries were imported to the Ansys® 16.02 geometry model to be recognized by the program; then, they were taken to the meshing module, where discretization of both models is performed, obtaining as a result the discretized models with elements of tetrahedral volume. Thereafter, the same parameters were defined for both meshes, which are relevance of 100; face sizing was applied on the chamber inlet and ring outlet, identified as the purple zones in Figs. 13a and 13b. Finally, the meshes were generated for each model, as seen in Fig. 14. After conducting a mesh study that evaluated different parameters, it was possible to determine that the independence of the results is obtained as of 4.5-million elements in the mesh configuration. Table 1 shows the best metrics obtained, which, in turn, guarantee homogeneity in the experiment. The final step named the boundaries, inputs, and outputs of the fluid to be identified later in the analysis module when conducting the respective configuration.

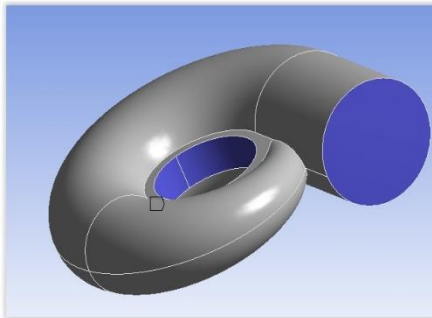


Figure 13a Inlet and outlet of the continuous chamber

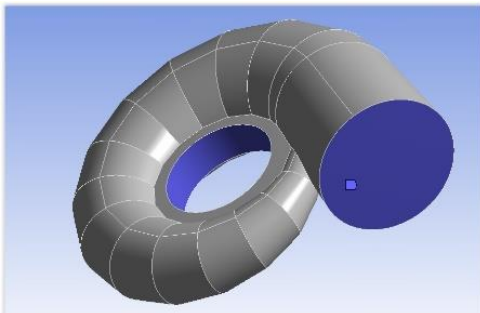


Figure 13b Inlet and outlet of the sectioned chamber

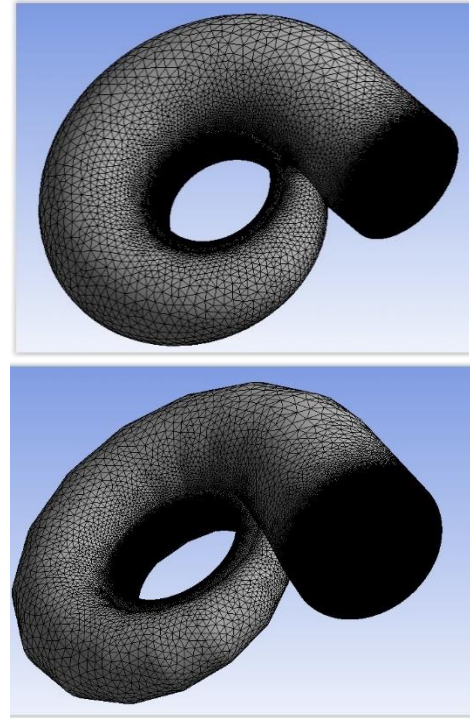


Figure 14 Meshed volumes of the continuous and sectioned chambers

Table 1 Metric data of the meshing of both spiral chambers

Metrics			
Chamber type		Continuous	Discrete
Nodes		860854	924957
Elements		4789661	5167964
Aspect ratio	Minimum	11.575	11.602
	Maximum	11.826	13.466
	Average	18.115	18.085
	Standard deviation	0.44533	0.44512
Obliquity	Minimum	3.31E-12	3.58E-05
	Maximum	0.84992	0.846
	Average	0.21316	0.21174
	Standard deviation	0.11423	0.11397
Orthogonal quality	Minimum	0.21042	0.18978
	Maximum	0.99705	0.99773
	Average	0.86727	0.86787
	Standard deviation	8.13E-02	8.16E-02

B2. Computational Fluid Dynamics

During the 1970s, Computational Fluid Dynamics (CFD) was used as an acronym to express the combination of physics, numerical mathematics, and computational sciences to use computational tools from fluids simulation.

[14]. By applying this technique, the hydrodynamic analysis is conducted of both spiral chambers in the CFX module of the Ansys® 16.02 software; wherein, the boundaries of the flow volumes are defined within the chambers. The conditions for both included domain of the environment (water) corresponding to the fluid within the chamber, with properties given by -4una reference pressure of 1 atm, given that for this case such is considered incompressible. Boundary conditions defined a normal velocity of 2 ms-1 and static pressure of 0 Pa at the ring outlet; the turbulence model selected was k-omega, based on prior studies on the theme by [15]. A model was established in stationary state with a limit of 1000 iterations to carry residues up to 10-4, to guarantee that calculation errors have the least possible significance. To guarantee equanimity in the results obtained, both simulations were developed in the same computer equipment, which has two Intel® Core i7-4770 processors with eight physical nuclei at 3.40 GHz, 12 Gb RAM memory, and a graphic processing unit (Nvidia® G-Force GT 460).

3. Results analysis and conclusions

To observe the results graphically in the post-processing of the simulations, the study used the methodology developed by [15], where a cylindrical revolution surface is generated that coincides with the turbine's outlet region. A set of plotted points is created of 360 angular positions and 21 axial positions (7560 in total). From each of these points the speed vector is obtained and its components on the X, Y, and Z axes. This information on the vector field flow at the turbine outlet is transferred to a database to process on MATLAB®. This graphic, in cylinder form, corresponds to the perimeter surface of a cylinder with a normal vector (radial) of velocity v_r , where through a computational code this cylinder is cut forming a film (tape) on a 2D plane. The velocity film was analyzed at 50%, 75%, and 100% of its central area, given that it there where it had the highest flow density and, hence, its analysis is more representative [16]. Supervised techniques searches adjustment to input data and in the specific case of neural networks this technique had the best performance allowing to verify that variables chosen were appropriate. In addition, identifying the viability of these variables allowed to develop an additional model of particle swarm, whose comparison will be included in a future work.

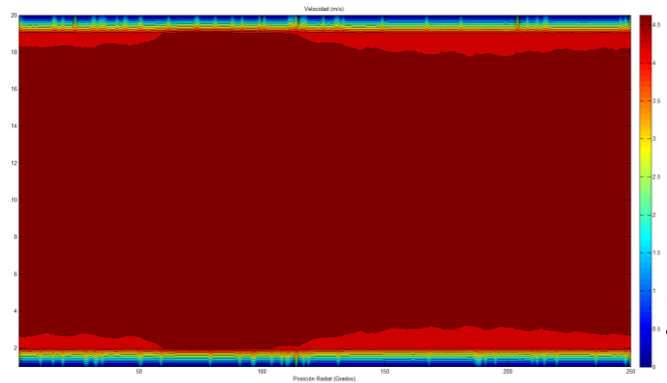
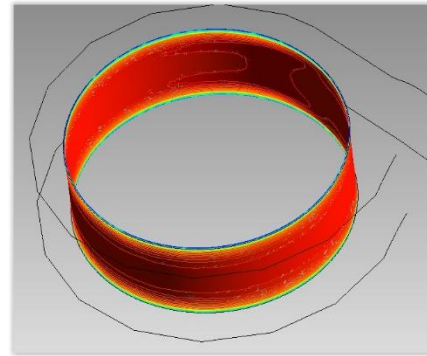


Figure 15a. Cylinder-shaped outlet; **Figure 15b.** Outlet in film form on a 2D plane

Upon implementing the methodology described to obtain the absolute, tangential, and normal velocity profiles of the flow on the outlet of the spiral chambers, the following results were obtained: analysis of 100% of the area of the output absolute velocity profile (Figs. 15a, 16a) and filtering of the border effects, thus, extracting 75% (Figs. 15b, 16b) and 50% (Figs. 15c, 16c). This code permitted generating 2D images of the velocity field and obtain qualitative information of the maximum, minimum, average, and standard deviation values of each velocity profile. The procedure described was applied to both spiral chambers.

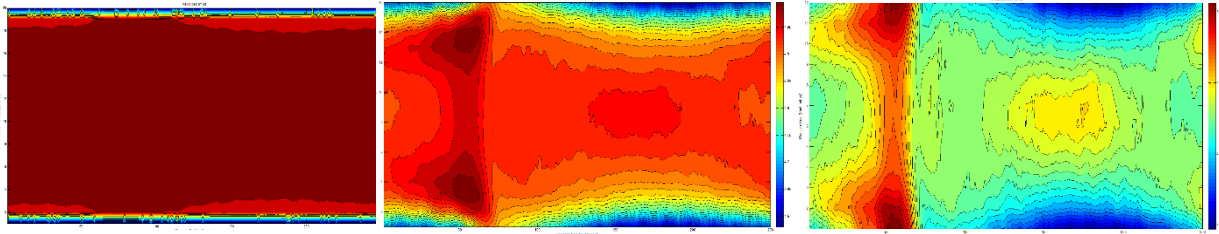


Figure 16a Total velocity 100%; **Figure 15b.** 75%; **Figure 15c.** 50%

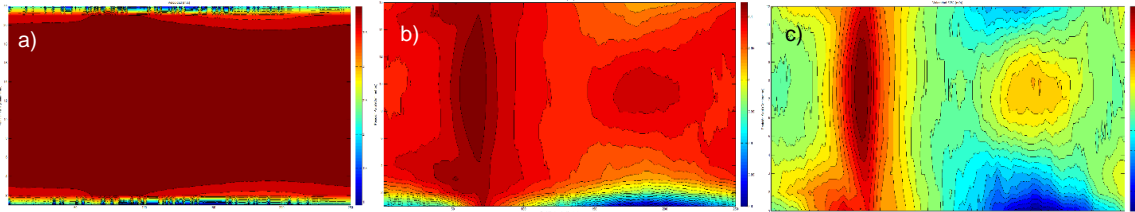


Figure 16a Total velocity 100%; **Figure 16b.** 75%; **Figure 16c.** 50%

To analyze the results, the average, maximum, and minimum mass flow velocities were taken as principal parameters at the outlet of the chambers, in normal manner and on the X, Y, and Z axes to provide validity to the

comparison. The results obtained were compared quantitatively amongst them and, likewise, a qualitative comparison was performed of the velocity profiles obtained (Table 2).

Table 2 Total velocity values for each spiral chamber.

	Velocidad	Velocidad x	Velocidad y	Velocity z	
Flujo masico absoluto	4.834e+00 [m s ⁻¹]	-7.759e-04 [m s ⁻¹]	3.930e-01 [m s ⁻¹]	2.021e-01 [m s ⁻¹]	Cámara seccionada
MaxVal	5.013e+00 [m s ⁻¹]	1.617e-01 [m s ⁻¹]	4.934e+00 [m s ⁻¹]	4.962e+00 [m s ⁻¹]	
MinVal	4.201e+00 [m s ⁻¹]	-1.550e-01 [m s ⁻¹]	-4.936e+00 [m s ⁻¹]	-4.947e+00 [m s ⁻¹]	
Flujo masico absoluto	4.015e+00 [m s ⁻¹]	1.797e-01 [m s ⁻¹]	-8.344e-04 [m s ⁻¹]	2.050e-01 [m s ⁻¹]	Cámara continua
MaxVal	4.136e+00 [m s ⁻¹]	4.084e+00 [m s ⁻¹]	2.019e-01 [m s ⁻¹]	4.107e+00 [m s ⁻¹]	
MinVal	3.269e+00 [m s ⁻¹]	-4.101e+00 [m s ⁻¹]	-2.071e-01 [m s ⁻¹]	-4.098e+00 [m s ⁻¹]	

Normal velocity values (Table 2) show, qualitatively and quantitatively, that the velocities are in close range, finding slightly higher velocities in the spiral-sectioned chamber. For velocities in the different axes (X, Y, Z), greater differences are present in the velocities obtained; in some cases presenting negative velocities, which would represent zones in the geometry with a high reduction in flow velocity and which the program interprets as negative values.

This study permitted identifying higher velocities in the outlet region of the spiral chamber if it is compared to the input region, as in other studies [4], [12]. Velocity contours at the outlet of the spiral chamber similar to those obtained by Zhu, which reach higher absolute velocities in the middle region of the chamber's radial outlet surface [8].

4. Conclusions

This work provides a comparative view of the performance between both manufacturing methods of spiral chambers, by availing of existing computational simulation tools.

An experimental phase is required with scale models to assess geometry against geometry, the effects generated on the fluid's behavior.

Further research is needed on the theme, as well as evaluation of new conditions closer to the real world, which generate more significant differences in the velocities

obtained, or that on the contrary reaffirm the results obtained in this research.

Although a difference exists when comparing the speeds between the spiral-sectioned chamber (higher speeds) and continuous chamber (lower speeds), the differences in the values obtained are not significant to give a final verdict, so that it is not feasible to determine a more optimal geometry for its application.

ACKNOWLEDGMENTS

The authors express gratitude to ITM, especially the Direction of Research through project P13143 “Modular systems of hydraulic microgeneration based on composite materials - Stage 1 – Characterization and evaluation of different types of micro-hydraulic turbines via numerical simulation” and the Department of Computer Systems for its support with hardware, software, and connectivity.

References

- [1] C. Mataix, Ed., *Turbomáquinas hidráulicas: turbinas hidráulicas, bombas, ventiladores*, 3rd ed. Madrid: ICAI, Editorial, 1975.
- [2] S. J. Williamson, B. H. Stark, and J. D. Booker, “Low head pico hydro turbine selection using a multi-criteria analysis,” *Renew. Energy*, vol. 61, pp. 43–50, Jan. 2014.
- [3] J. D. Canales Rivas, Antonio José; Mariona Gómez, “Métodos de diseño hidráulico de turbinas francis para pequeñas centrales hidroeléctricas,” UNIVERSIDAD CENTROAMERICANA JOSÉ SIMEÓN CAÑAS, 2014.
- [4] H.-J. Choi, M. A. Zullah, H.-W. Roh, P.-S. Ha, S.-Y. Oh, and Y.-H. Lee, “CFD validation of performance improvement of a 500 kW Francis turbine,” *Renew. Energy*, vol. 54, pp. 111–123, Jun. 2013.
- [5] R. López, “TRABAJO ESPECIAL DE GRADO DISEÑO DE CAJAS ESPIRALES DE SECCIÓN CIRCULAR PARA,” Universidad Central de Venezuela UCV, 2003.
- [6] A. M. Fuller and K. V. Alexander, “Exit-flow velocity survey of two single-tangential-inlet vaneless turbine volutes,” *Exp. Therm. Fluid Sci.*, vol. 35, no. 1, pp. 48–59, Jan. 2011.
- [7] P. K. Maji and G. Biswas, “Three-dimensional analysis of flow in the spiral casing of a reaction turbine using a differently weighted Petrov Galerkin method,” *Comput. Methods Appl. Mech. Eng.*, vol. 167, no. 1–2, pp. 167–190, Dec. 1998.
- [8] H. Zhu, R. Zhang, G. Luo, and B. Zhang, “Investigation of Hydraulic Characteristics of a Volute-type Discharge Passage based on CFD,” *Procedia Eng.*, vol. 28, pp. 27–32, 2012.
- [9] G. A. Aggidis and A. Židonis, “Hydro turbine prototype testing and generation of performance curves: Fully automated approach,” *Renew. Energy*, vol. 71, pp. 433–441, Nov. 2014.
- [10] X. PENG, Z. YANG, S. LIU, and X. JU, “Equivalent pipe algorithm for metal spiral casing and its application in hydraulic transient computation based on equiangular spiral model,” *J. Hydrodyn. Ser. B*, vol. 26, no. 1, pp. 137–143, Feb. 2014.
- [11] L. Wang and D. Wei, “The Optimum Structural Design for Spiral Case in Hydraulic Turbine,” *Procedia Eng.*, vol. 15, pp. 4874–4879, Jan. 2011.
- [12] P. Newton, C. Copeland, R. Martinez-Botas, and M. Seiler, “An audit of aerodynamic loss in a double entry turbine under full and partial admission,” *Int. J. Heat Fluid Flow*, vol. 33, no. 1, pp. 70–80, Feb. 2012.
- [13] Ansys®, «11.1.1. Discretization of the Governing Equations», 2014.
- [14] Blazek Jiri, de Computational Fluid Dynamics: Principles and Applications, Waltham: Helsevier, 2015.M. C.
- [15] Juan Pablo Mejía Rico, Jonathan Graciano-Uribe, David Steeven Villa, Juan José Arbeláez Toro, Diego Hincapié-Zuluaga, Estudio computacional fluido dinámico de cámaras en espiral aplicadas a la generación de energía hidráulica a micro escala, X CONGRESO COLOMBIANO DE MÉTODOS NUMÉRICOS: Simulación en Ciencias y Aplicaciones Industriales, 2013.
- [16] Henry, Pierre, *Turbomachines Hydrauliques*, Presses Polytechniques et Universitaires, Romandes, Suiza; 1992.

